Solar and stellar measurements using accurate spectroscopic techniques: Final report for the 2013 ΣΠΣ Undergraduate Research Award

Main Contributors: Sara-jeanne Vogler (Team Leader), Keeley Townley-Smith, Jamie Fairchild, Jose Castro, Susan Salazar

Collaborators: Jacob James, Aaron Weatherford, Jessica Plaia, Bryan Neal

(Dated: December 30, 2013)

Department of Physics, Lamar University, Beaumont, Texas

Faculty Advisor:
Cristian Bahrim

SPS Chapter #3643 Officers:
Jacob James (President)
Jason Dark (Vice President)
Danielle Dark (Treasurer)
Keeley Townley-Smith (Secretary)

CONTENTS

I. Initial Objectives of the Proposal 4

II. Experimental Investigation 4

III. Experimental Set-up 6

A. HRD Set-up 6

B. APSL Set-up 7

C. PEA Set-up 7

IV. Procedures and Data Acquisition 7

A. HRD Procedures and Data Acquisition 8

B. APSL Procedures and Data Acquisition 9

C. PEA Procedures and Data Acquisition 11

V. Analysis 15

A. HRD Analysis 15

B. APSL Analysis 19

C. PEA Analysis 23

VI. Results and Conclusions 24

A. HRD Conclusions 24

B. APSL Conclusions 24

C. PEA Conclusions 24

VII. Future Work 25

A. HRD Future Work 25

B. APSL Future Work 25

C. PEA Future Work 25

VIII. Expenses 25

References 26

A. Expense Detail 28

B. Research Presentations 29

1. South Central Conference for Undergraduate Women in Physics (University of Texas at Austin, 2013) 29
2. Joint Spring 2013 Meeting of the Texas Sections of the APS, AAPT, SPS 30
3. Texas Undergraduate Research Day at the Capitol in Austin, Texas 32
4. Joint Fall 2013 Meeting of the Texas Sections of the APS, AAPT, SPS 34

I. INITIAL OBJECTIVES OF THE PROPOSAL

Hertzsprung-Russell Diagram (HRD): Generate a Hertzsprung-Russell Diagram, using blackbody curves of radiancy for the most visible stars in the northern night sky.

Analysis of Polarized Stellar Light (APSL): Analyze the polarization of light emitted from very bright stars and the Sun, due to the shape of the stars; and study the effects of the optical components of the telescope.

Pollutants in Earth's Atmosphere (PEA): Identification in the solar spectrum the absorption spectra of the gaseous components located in the Earth's and Sun's atmospheres.

II. EXPERIMENTAL INVESTIGATION

As it will be explained further, the experiments have been re-assessed and changes have been implemented with the purpose of reaching our initial commitment from the proposal. For clarity sake, a summary of the changes will be provided in Sections III and IV.

The atmospheric conditions and architectural disadvantages experienced during early trials led us to some revisions of our initial proposal. Our experiments needed a rooftop excursion in order to collect data from the daytime and nighttime skies. After our first time collecting data outside in February, the complications of moving our equipment were realized, including getting the equipment through the rooftop hatch shown in Figure 1. The light pollution on the roof was another major challenge in getting accurate data and effectively eliminating the background noise. Every attempt to block the background light, from portable shields to tents, proved to have lead toward more complications.

FIG. 1. Photo of the Rooftop access[1]

Therefore, our innovative team adopted a method for performing all of the experiments from the proposal in a closed laboratory environment. We simulated the star light and the Sun using various light sources, including light bulbs and a Bunsen burner. Our goal was to keep the richness of the experiment without degradation of the learning experience.

HRD: To simulate our stars, we enclosed light bulbs, thus simulating a blackbody at

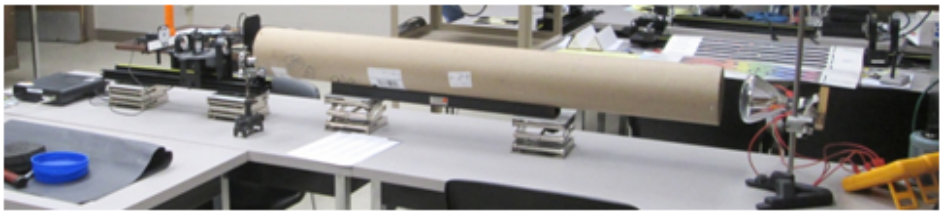

FIG. 2. Simulated Blackbody Set-up

thermal equilibrium. For the simulation of non-equilibrium stars, we used a Bunsen burner. Figure 2 shows the light source introduced in our experimental setup. Due to several difficulties (i.e. the weather conditions, the fragility of the equipment and the hazards in carrying it using the rooftop access), we decided to develop a version of our experiment in lab. For running a clean data acquisition, we planned to use a fiber optics. Building up the fiber optics adapter for the telescope took us much longer than initially anticipated. When it was completed (in late October), we experienced constantly overcast skies in our area, and high humidity, damaging the transparency of our sky.

Transparency is used in astronomy for describing sky clarity. In its simplest form, transparency can be defined as the magnitude of the dimmest star to be seen with the naked eye. It is primarily affected by particles in the air and light pollution. Light pollution is always a factor in Beaumont, but high humidity also effects transparency and that is an oscillating weather factor here.[2]

Using the Bunsen burner light source, a blackbody-like curve was generated by using light from three different regions of the flame (top, middle, and bottom).

APSL: Initially, we wanted to take measurements of several bright stars and the Sun and observe the effects of polarization due to their shape. Assuming that all of these light sources were spherical, we would expect to observe the same results for each stellar object. The initial goal of this experiment was to test how the intensity of that light would change as we rotated the degree of polarization using light sources of different shapes. We accomplished this task by using a circular shaped source as our control case and a square-shaped polygon source as our test case for assessing our theory.

PEA: During the trials and errors in the earlier months of this project, we determined that the absorption spectra embedded in the solar blackbody spectrum would not be strong enough to produce an analyzable signal. This is largely due to the equipment available in

our budget and the complications of our atmosphere's composition due to surround chemical plants. Instead we chose to show the results of our theory in a controlled environment using a known blackbody source, as in APSL and HRD, and discharge tubes of several known gases. In this way, we would be able to show the absorption of the medium in which the light travels.

III. EXPERIMENTAL SET-UP

For the three experiments (HRD, APSL, and PEA), a similar experimental set-up has been used. This set-up is comparable to the one currently used in Lamar University's advanced optics course[3] shown in Figure 3. All three experiments used basic PASCO® equipment (http://www.pasco.com/home.cfm). A light shield would have been needed for outdoor measurements, but the design was never perfected due to our decision to perform indoor experiments.

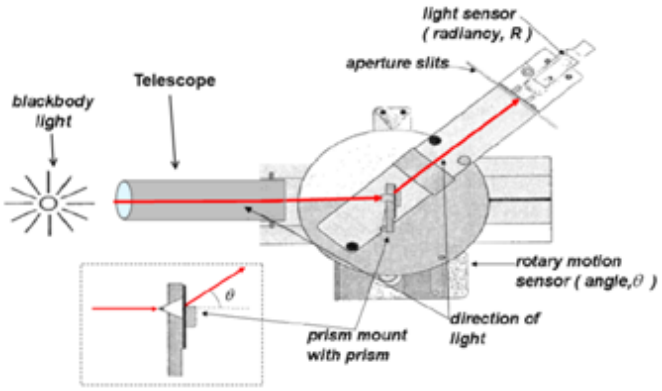

FIG. 3. A setup for the study of the blackbody radiation spectrum. The path of the light is shown by the two red arrows.[3]

A. HRD Set-up

We simulated a blackbody source with a long tube and light bulbs as shown in Figure 2). The Bunsen burner was used for simulation of light sources in non-(thermal) equilibrium. We used a variety of light sensors required for the range of temperatures of the sources we were studying. After preliminary trials we decided to use a single 90 mm Meade ETX-90EC Astro Telescope. Our studies indicated that field data would have to be collected using a fiber optic

FIG. 4. Bench-Tripod Adapter

support for the transport of the light from light source to the aperture slit of the detection system shown in Figure 3. The optical fiber was purchased and an adapter was built to hold it against the telescope. An adapter was fashioned to attach the fiber to the optics bench (Figure 4). The optics bench is thereby made more versatile and adjustable.

B. APSL Set-up

Similarly as in Figure 3. The only difference is the placement of two polarizers on the PASCO® bench as shown in Figure 5.

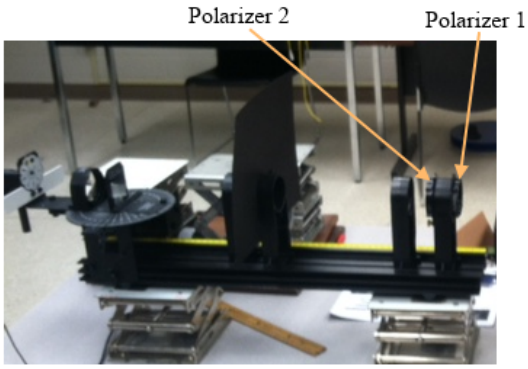

FIG. 5. Placement of the polarizers in the APSL set-up.

C. PEA Set-up

The same optics bench has been used for this experiment as for the HRD experiment. The source was restricted to a light bulb, with adjustable brightness due to the variable transformer to which it was connected. Different substances such as nitrogen, hydrogen, and sodium were placed in front of the bench, along the optical axis. The data was collected, as we did with the HRD.

IV. PROCEDURES AND DATA ACQUISITION

While the first measurements began in February 2013, the majority of them did not occur until September 2013. The interim period, from March to August, was primarily spent calibrating the equipment, learning to use the DataStudio® software, and searching for better experimental techniques for each of the projects.

The following sections report the raw data and procedures by which it was obtained.

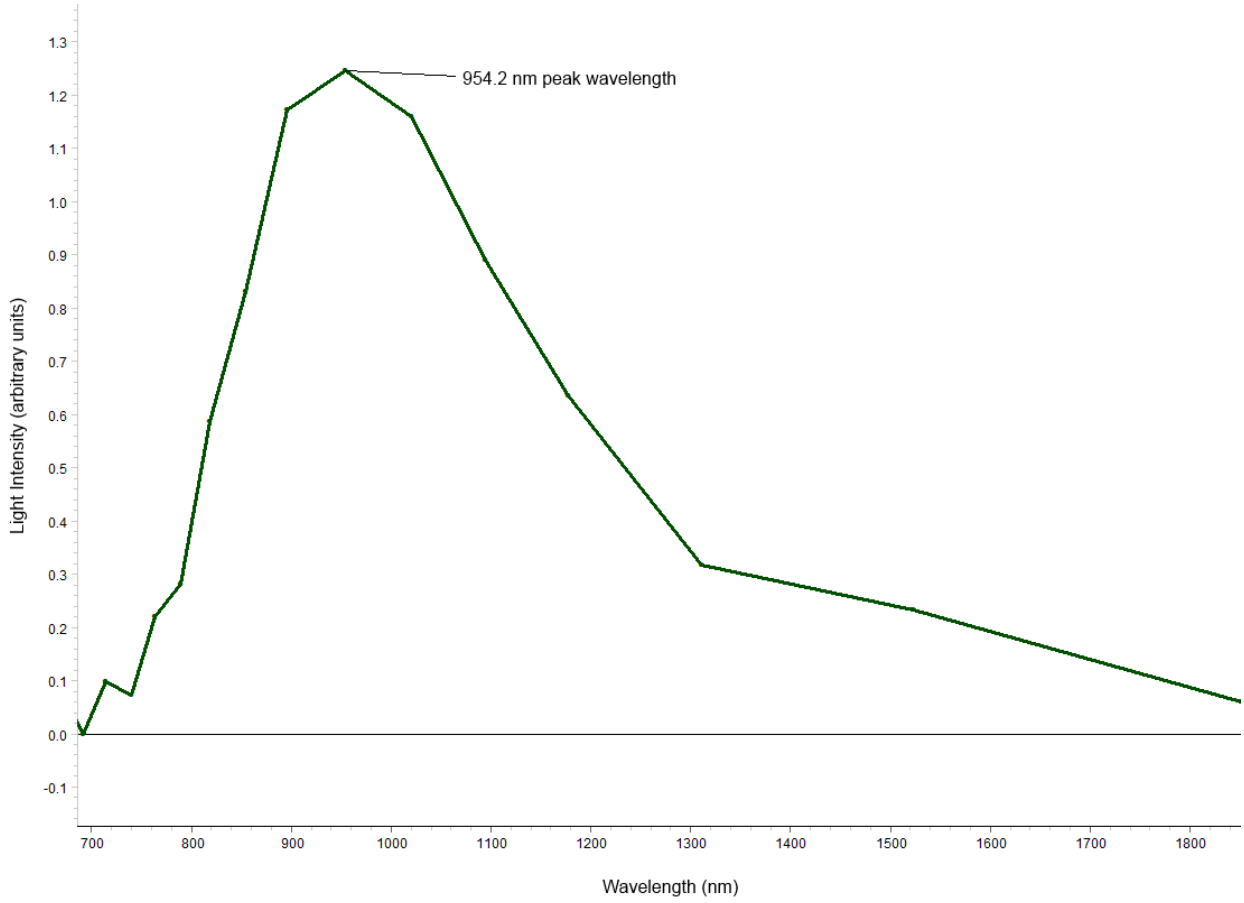

FIG. 6. A typical DataStudio® run for a simulated star.

A. HRD Procedures and Data Acquisition

The first data collection was attempted the night of February 28th. At that time, data was not successfully gathered for the purpose of quantitative measurement, but the issues that should have been addressed before accurate data could be collected were identified.

Throughout the remaining part of the year, we attempted to simulate in lab a red giant, a blue dwarf, and some of the main sequence stars. Since the top of the flame is considered the coolest and brightest part of the flame, we expect to simulate a bright cool star, with the use of red wavelength filters, similar to a Red Giant. As one would expect, the bottom of the flame is the hottest and dimmest part. Therefore, a Kodak blue filter was used to eliminate all colors but blue, and thus to reproduce a curve similar with that from a hot dim star, such as a Blue Dwarf. Finally, the middle part of the flame has a mixture of qualities present in both the top and bottom parts of the flame. It is for this reason that

the blackbody curve generated with this procedure is expected to be similar to that of the Main Sequence stars like our Sun.

Twenty-seven readings were recorded each generated using a different settings such as a certain height along the flame, use of appropriate filters, and the gas flow from a Bunsen burner. The data was recorded in DataStudio® as near-equilibrium Planck-type distribution, with the maximum corresponding to the wavelength used to determine the temperature of the flame. The intensity for each flame was estimated using the area under this peak. A sample peak is shown in Figure 6. Table I shows the peak wavelength and raw intensity of the 27 simulated stars.

B. APSL Procedures and Data Acquisition

Using the set-up described above, data was collected using DataStudio® for the two different shapes of simulated blackbody sources, see Figure 7. Temperature of the source was adjusted and changed by varying voltage until a temperature was established for an optimum signal, meaning that the peak of the curve was not so intense that it is well-defined and clearly visible from the test runs as shown in Figure 8. This temperature was maintained for each source. Data was collected at 0, 20, 40, and 60 degree orientations for both sources with a polarizer, as well as one run without a polarizer to be used as a reference. The raw signals from both experiments are shown in Figure 8 and Figure 9. These two graphs are color coded similarly, for consistency and easy reading. Since we were not able to calculate the area under the curve using an integral in DataStudio®, the data was exported to Excel^{TM} as a text file and calculations were done in Excel^{TM}, which will be described in more detail in Section V B on page 19.

FIG. 7. Shape of the polygon blackbody source. The second shape is circular.

TABLE I. The Wavelengths at the Peak of Radiancy and the Relative Intensities of 27 Simulated Stars

	Max wavelength (nm)	**Temperature (K)**	**Relative Intensity (arbitrary units)**
Star 1	908.48	3189.68	779.36
Star 2	1072.06	2703.00	708.94
Star 3	954.22	3036.79	646.20
Star 4	949.33	3052.45	92.21
Star 5	1207.17	2400.46	338.94
Star 6	929.71	3116.86	160.07
Star 7	920.73	3147.24	211.57
Star 8	929.71	3116.86	203.99
Star 9	903.56	3207.06	196.83
Star 10	938.96	3086.15	246.43
Star 11	895.33	3236.52	171.21
Star 12	879.56	3294.58	124.37
Star 13	925.19	3132.09	148.22
Star 14	920.73	3147.24	169.66
Star 15	903.56	3207.06	154.94
Star 16	887.34	3265.69	218.65
Star 17	938.96	3086.15	144.41
Star 18	920.73	3147.24	144.44
Star 19	923.34	3138.34	149.07
Star 20	883.42	3280.17	144.23
Star 21	879.56	3294.58	180.94
Star 22	958.34	3023.73	168.46
Star 23	912.02	3177.30	160.02
Star 24	891.31	3251.14	202.20
Star 25	948.50	3055.11	147.23
Star 26	887.34	3265.69	151.36
Star 27	925.19	3132.09	265.13

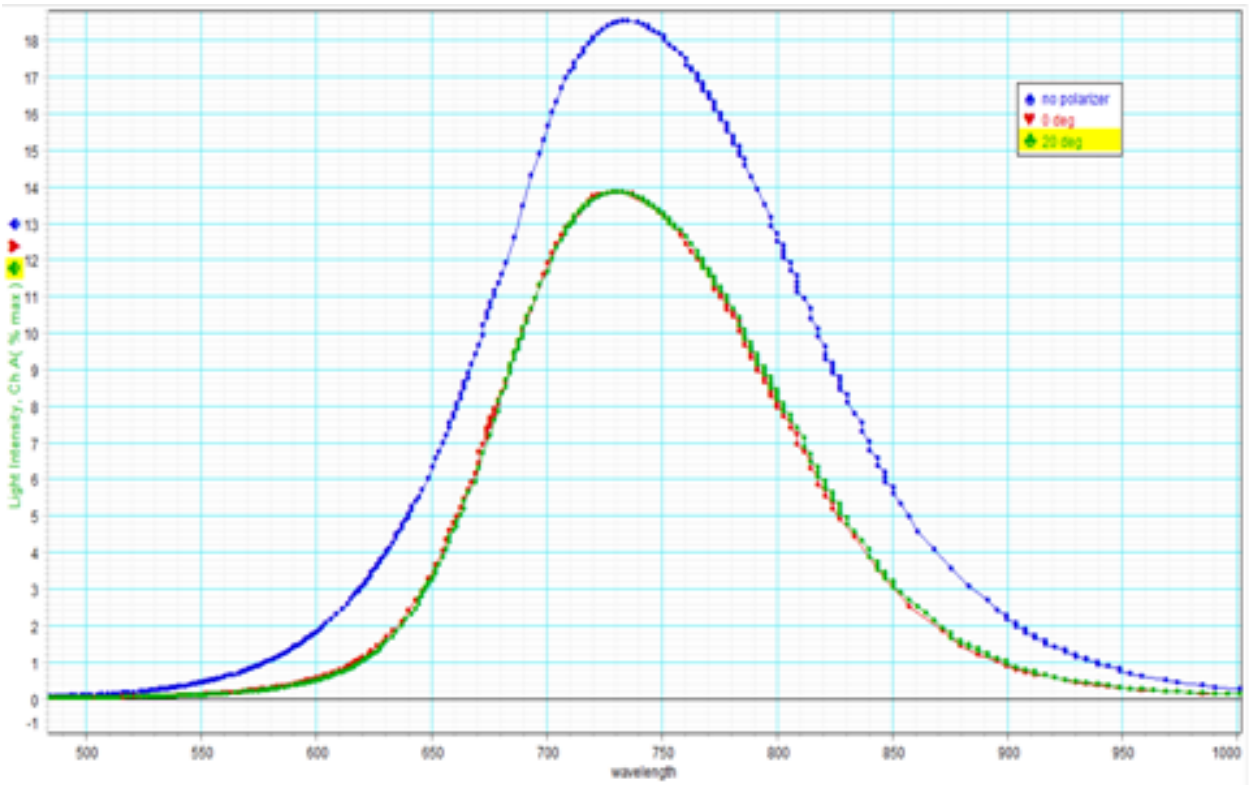

FIG. 8. Light signal as detected by DataStudio® for studies of the polarization of light from a Circular light source

C. PEA Procedures and Data Acquisition

From spectroscopic data acquired during the early months of 2013, we were able to determine the characteristic wavelengths of various elements present in the Sun's photosphere and the Earth's atmosphere assessed and used for this section of the project. Throughout the year we continuously gathered spectra for various elements.

This experiment began by using the data obtained from these spectroscopic projects. The spectra for hydrogen, nitrogen, oxygen were composited with a spectrum of air to better understand how elements combine into compounds, see Figure 10. We also developed a deep understanding of helium (Figure 11), argon, and carbon, among other elements. We validated our findings by comparing this data with the NIST Database[6].

The spectra reported in Figures 10 and 11 provide the characteristic wavelengths for the some of the most relevant elements in the absorption spectra embedded in the blackbody spectrum of Sun. These elements, and others as listed in Table II, have been used in our

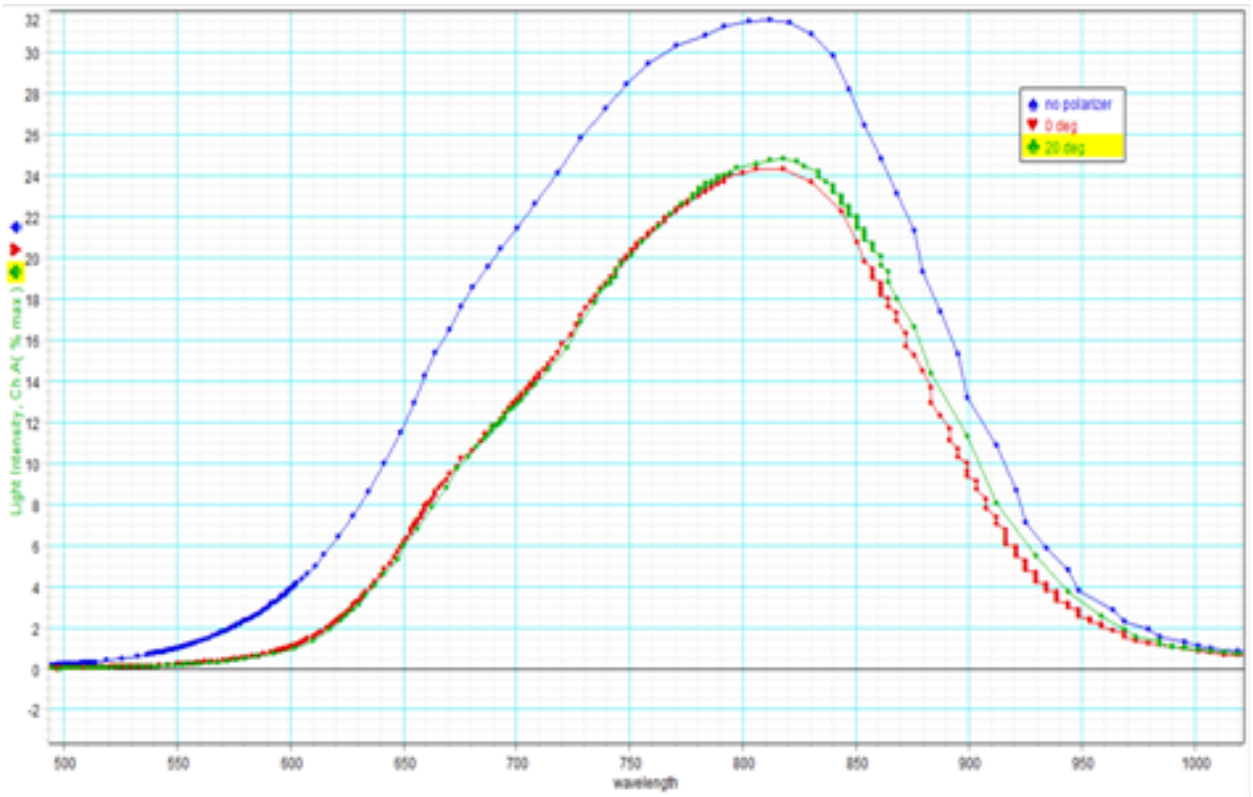

FIG. 9. Light signal as detected by DataStudio® for studies of the polarization of light from a Polygon light source

experiments and simulations. A typical spectrum includes a set of Lorentzian profiles corresponding to the wavelengths characteristic to different elements. Pressure broadening causes the Lorentzian features to widen, making a Gaussian approximation appropriate. For the simulation of emission lines with pressure broadening caused by atomic collisions we used

$$y = I \frac{\left(\frac{\Gamma^2}{4\hbar^2}\right)}{\left(\frac{\Gamma^2}{4\hbar^2}\right) + (x-\lambda)^2}, \tag{1}$$

such that the x-axis is the wavelength and the light intensity is along the y-axis. Lambda (λ) is the characteristic wavelength according to the NIST database, Γ is the full width at half maximum (FWHM) and indicates the lifetime of the excited state from where the characteristic wavelength is emitted (in our case Γ is an arbitrary value to widen the peaks), and I is the scaling factor for the height of the peaks. The scaling factor, I, is determined by R, the ratio of each particular element as listed in Table II, and I_λ and I_{max}, the intensity of a characteristic wavelength and the maximum intensity for the characteristic wavelengths of that particular element, respectively, as listed in the NIST Database[6]. The scaling factor

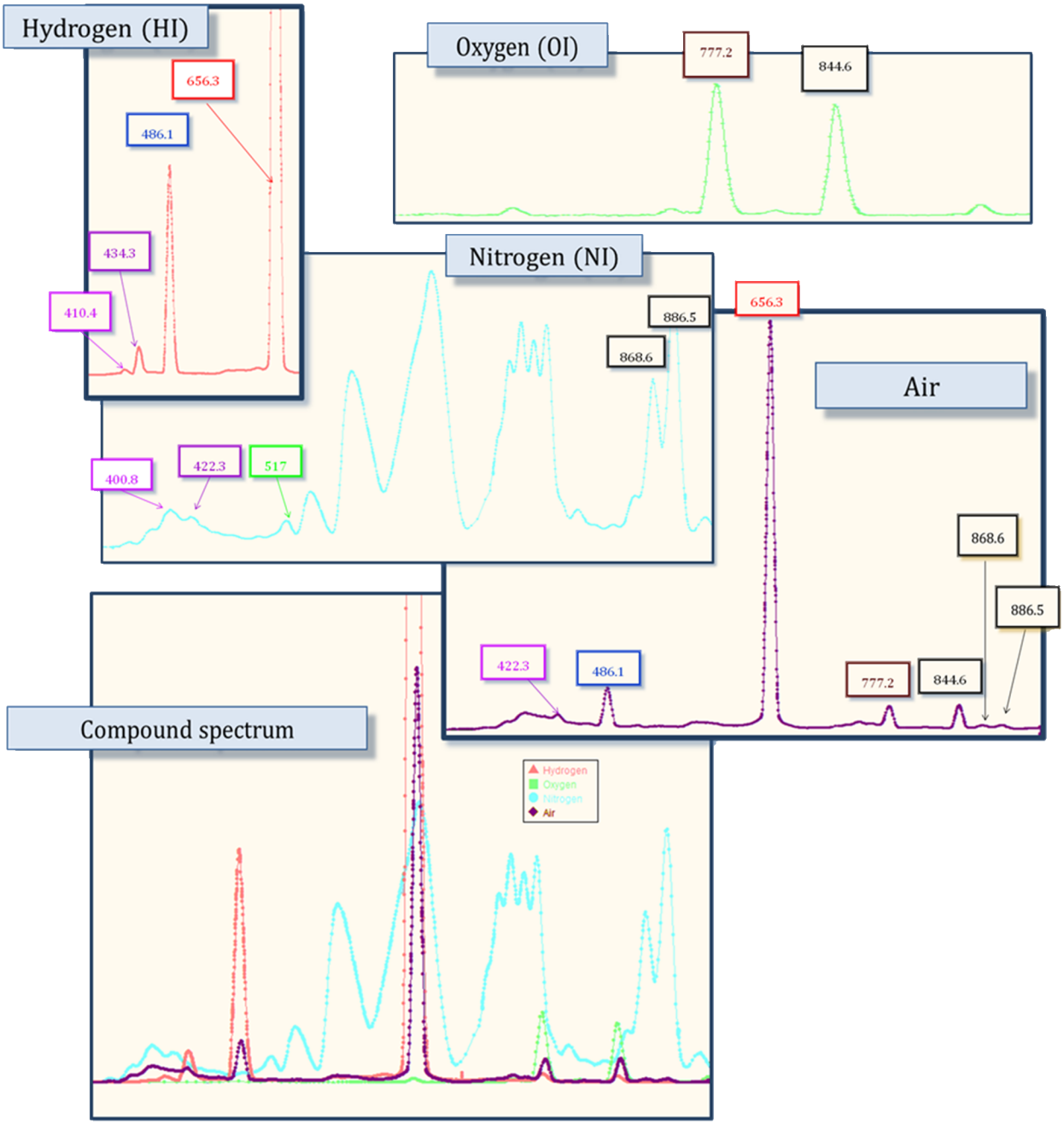

FIG. 10. Hydrogen, oxygen, nitrogen, and air composite spectra as reported at the Joint Fall 2013 Meeting of APS, AAPT, and SPS in Brownsville, Texas[4].

is given by the formula

$$I = R * \frac{I_\lambda}{I_{max}}. \tag{2}$$

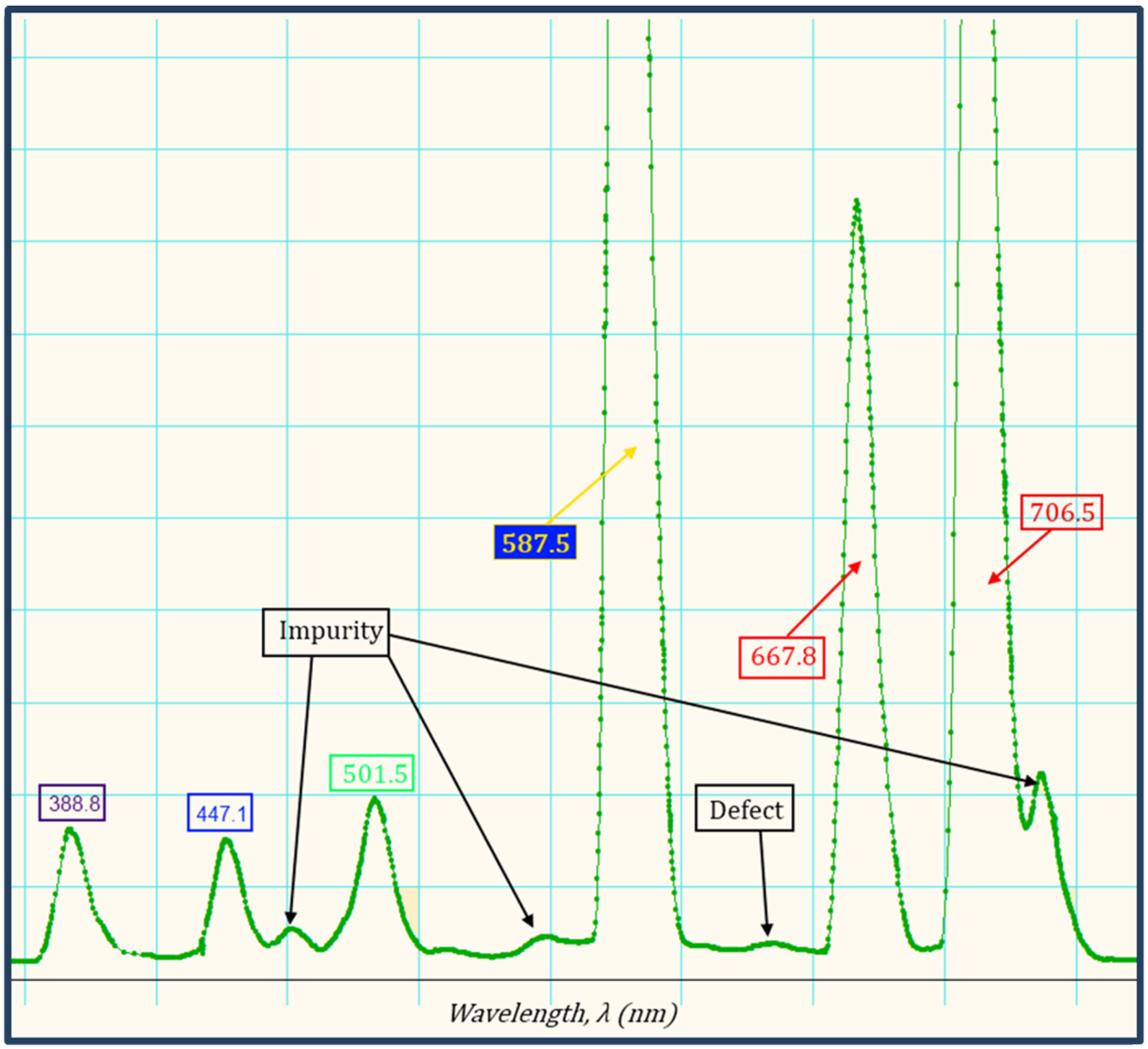

FIG. 11. Helium spectrum reported at the 2013 South Central Conference for Undergraduate Women in Physics in Austin, Texas[5].

The background intensity was provided using the Planck formula for radiancy

$$R(x) = \left(\frac{c}{4}\right)\left(\frac{8\pi}{x^4}\right)\left(\frac{hc}{x}\right)\left(\frac{1}{e^{\left(\frac{hc}{xkT}\right)}-1}\right). \tag{3}$$

The Lorentzian peaks, y, from Formula 5, were than subtracted from the Planck curve using MATLAB®.

A sodium lamp was used in the laboratory runs. This case is important because of several reasons: [1] the strongest transition is at 589 nm, in the middle of the visible range, where the VIZ detectors are the most sensitive, [2] the transition is from the first excited state to

the ground state of sodium, and therefore, in absorption it is the most likely to be detected, and [3] the probability amplitude is large. The theoretical curve based on a blackbody source with a temperature of 3977 K (as measured using the temperature dependence of resistivity of the tungsten filament) was produced by MATLAB® as shown in Figure 12. We recorded the curves shown in Figure 13 using DataStudio®. In Figure 13, the Planck curve has a maximum at 865 nm wavelength.

A theoretical curve for our PEA experiment, was produced in a similar fashion as the sodium curve, as to gain the appearance of the example in Figure 1a of our proposal, shown as an insert to Figure 14 in this report. We assess the absorption caused by various elements present in the blackbody spectrum from the volume of each layer of Earth's atmosphere[7], the Sun's photosphere, and the Sun's corona[8] considering the abundance of each element present in these layers, as reported in various academic and NASA sources[9–11]. The resultant values are reported in Table II. The labels listed in the table represent selected characteristic wavelengths reported in Figure 14.

In Figure 14 we show the theoretical Planck curve produced in MATLAB® for a temperature of 5778 K[11].

V. ANALYSIS

Data was analyzed for each experiment using Microsoft® Excel^{TM}, MATLAB®, and DataStudio®.

A. HRD Analysis

We experimentally took our maximum wavelength from each run by reading the position of the tallest peak in our wavelength vs. radiancy curves like the graph shown in Figure 6. We used Wien's Law to estimate the temperature of an ideal blackbody associated to that particular wavelength. Wien's law states that the wavelength and temperature of a blackbody are related through the equation

$$\lambda_{max} T = 2.8977685 \times 10^{-3}. \tag{4}$$

Then, we used the Stephan-Boltzmann Law,

$$I = \sigma T^4, \tag{5}$$

TABLE II. Elemental Composition of the Solar and Terrestrial Atmospheres

Element	Labels	% of Total
Ar		0.008337432%
C		0.032781934%
Fe	433 nm [a]	0.004260409%
H	389 nm - [b]	90.130373459%
	486 nm - [c]	
	656 nm - [d]	
	1094 nm - [e]	
	1282 nm - [f]	
He	588 nm [g]	8.807155788%
	1700 nm [h]	
	1870 nm [i]	
Kr		0.000000044%
Mg		0.003467774%
N	744 nm [j]	0.709963637%
	824 nm [k]	
	841 nm [l]	
	842 nm [l]	
Ne	706 nm [m]	0.011097565%
O		0.287905234%
S		0.001486188%
Si		0.003170537%

with σ in units of $W \cdot K^4/m^2$ to calculate the expected intensity of the glowing objects between 2500 and 100,000 K, if they would be comparable to a Main Sequence star. A plot of these results is in Figure 15.

In order to evaluate experimentally the intensity of each simulated "star", we imported the data into Excel and approximated the area under the curve using the Trapezoidal Rule, as also done in APSL, and scaled it according with Stephan-Boltzmann Law.

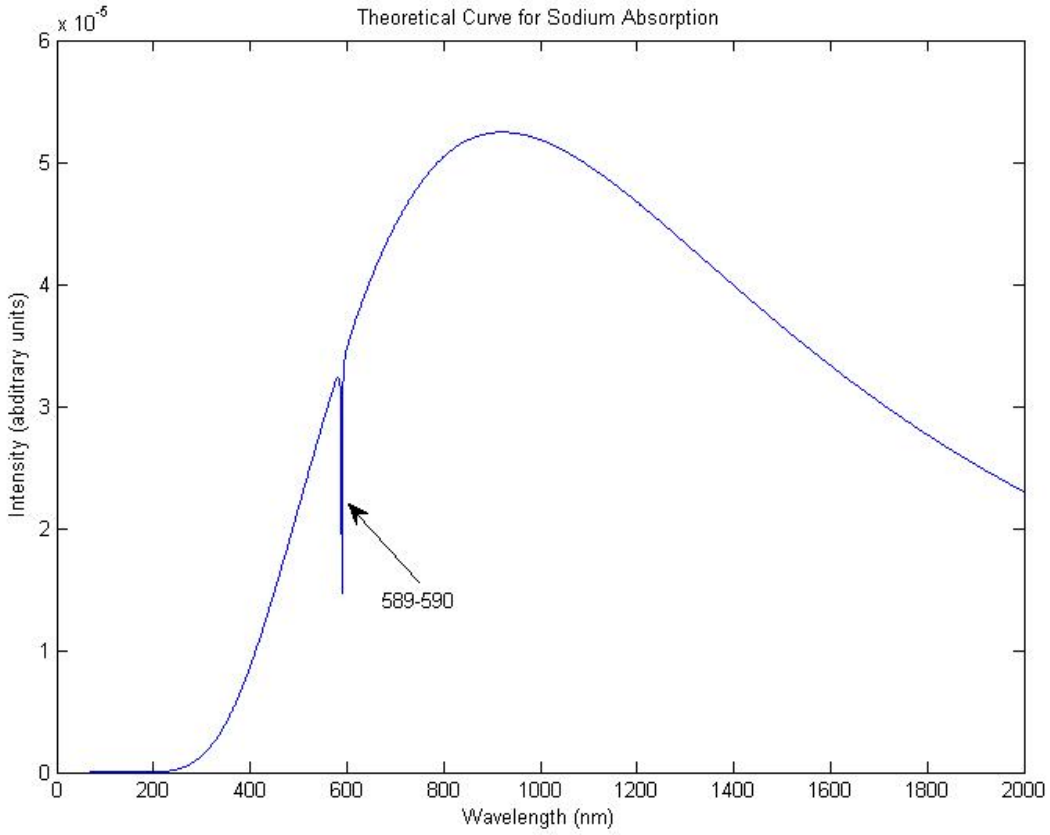

FIG. 12. Sodium Theoretical Curve from MATLAB® derivation.

Finally, we plotted all our 27 simulated stars against the horizontal diagonal given by the Stephan-Boltzmann Law for the main sequence stars in thermal equilibrium, as shown in Figure 16.

Our 27 stars are placed close or along the main sequence line. (One can see that the cluster to the bottom left is very close to the main sequence line, too, considering the scale around 3400 K.) It makes sense that we did not get any red giants because red giants are 10^{10} times more massive than regular main sequence stars and the ability to reproduce this intensity in our lab is not possible. Blue dwarfs would have been even more challenging as we would have to get up to temperature of 6000 K to peak in the blue part of the spectrum, comparable to those stars, while maintaining a low intensity. In conclusion, our data shown in Figure B is consistent with the established conditions of temperature in our flame.

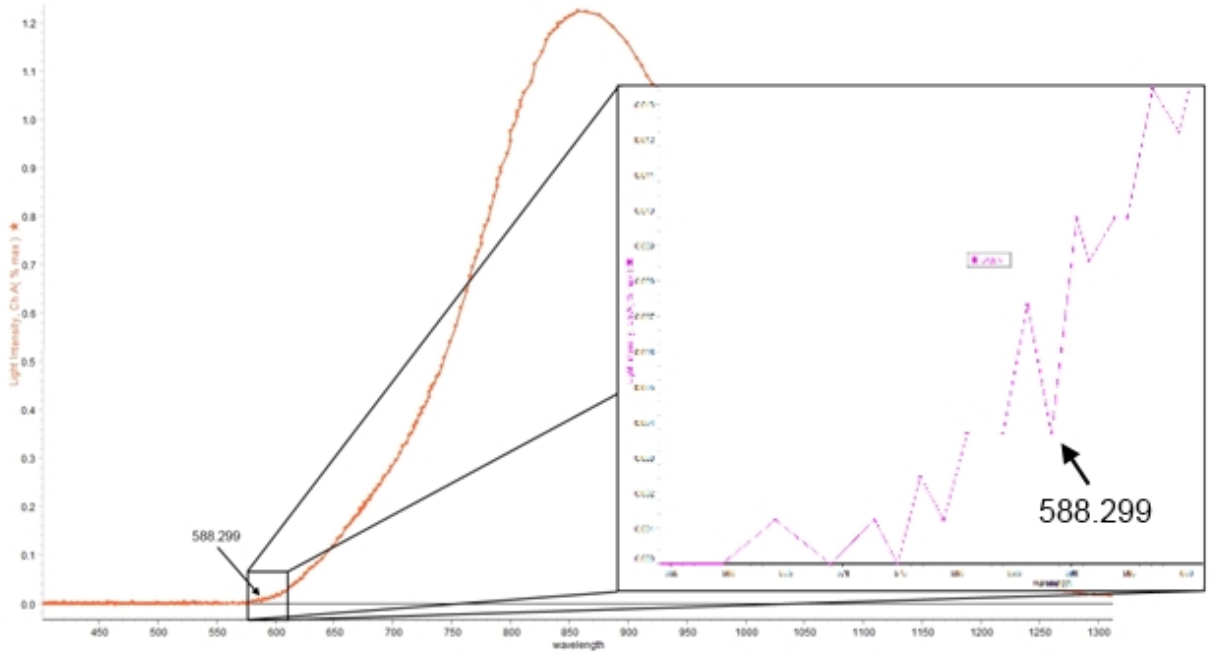

FIG. 13. Sodium raw data from DataStudio®, with a zoom on the expected region of interest.

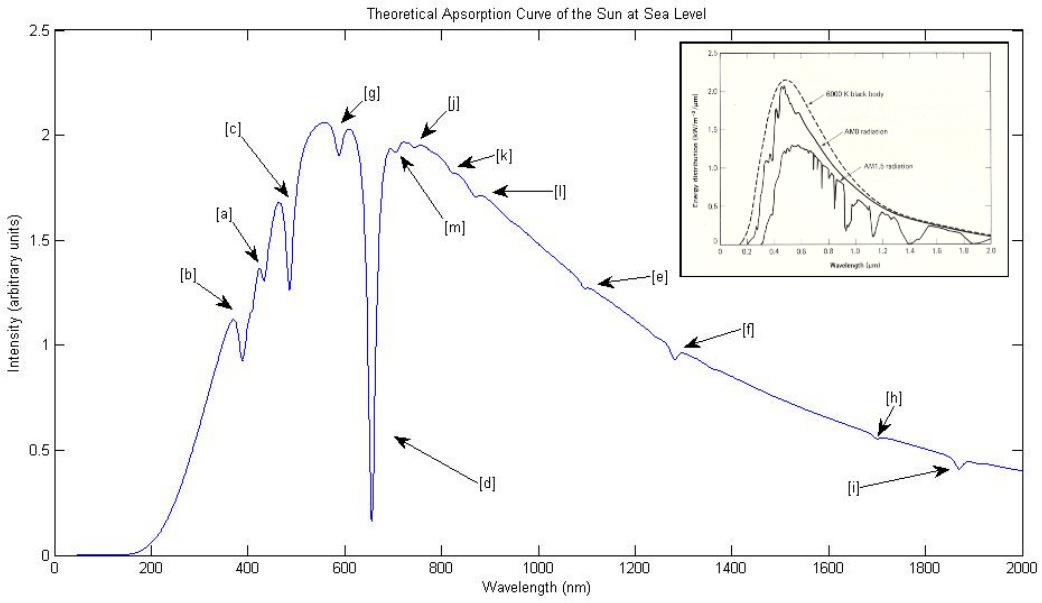

FIG. 14. MATLAB® produced curve of the Sun's blackbody with absorption lines theorized for the elements in the Earth's and Sun's atmosphere. The insert is from the proposal. One can notice the similarity between the location and allure of our absorption peaks and those in the inset from reference[12].

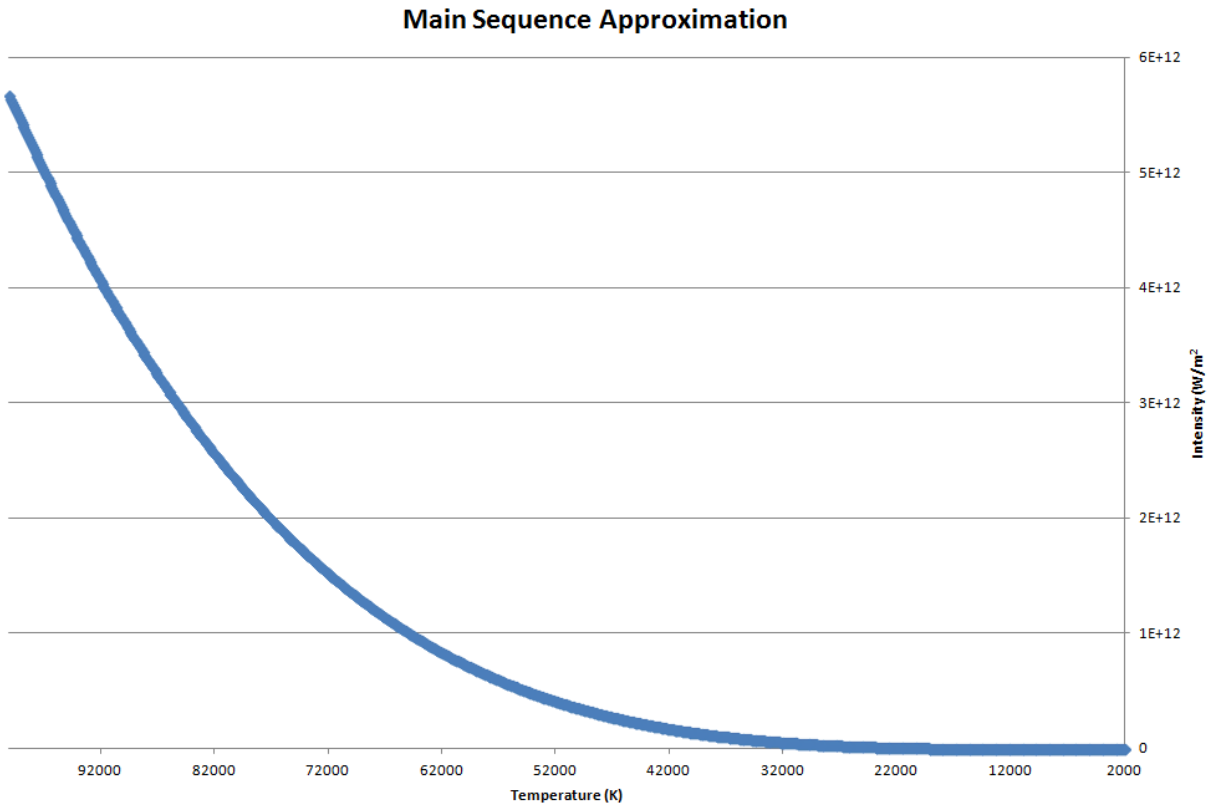

FIG. 15. The Intensity vs. Temperature of Main Sequence stars, as determined by using the Stefan-Boltzmann Law.

B. APSL Analysis

As mentioned above, the raw data was imported into Excel^{TM} as a Text File as shown in Table III. After that, we approximated the overall intensity which is given by the area under the curve using a rendition of the Midpoint rule and Trapezoidal rule. The calculated intensity from both methods was in agreement to at least the thousandths place, verifying the validity of both methods.

The intensity was calculated for the case without the polarizers, as well as the 0, 20, 40, and 60 degree orientation between the transmission axes two polarizers for both the polygonal and circular light sources, shown below in Tables IV and V. In Tables IV and V we compare the percentage change in the intensities of light polarized when the polarizer is rotated by increments of 20 degrees. This result is a convincing test that our experiment is done with good precision, since a rotation by the same increment makes the sequential cases to indicate the same percentage shift. The deviation from an exact $cos^2(20°)$ value

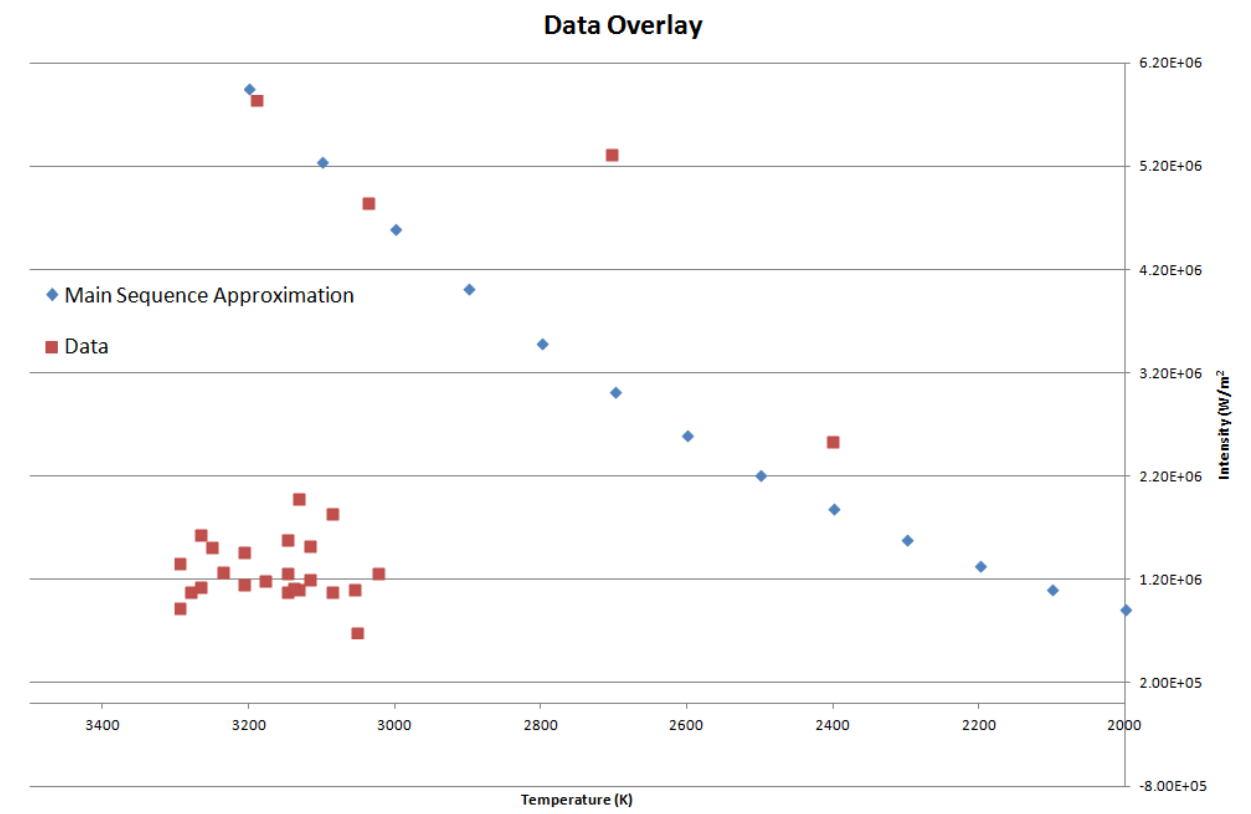

FIG. 16. A selected region from Figure 15 using data from our simulated stars.

indicates the departure from an ideal polarizer case.

In theory, we should expect a 50% decrease in intensity when we add an ideal polarizer in front of our source along the optical axis. In our case, for both the circular and polygonal case, we only observe a 31-35% drop in intensity. This is most likely due to the fact that we do not use ideal polarizers. Therefore, we can speculate that the polarization of light may be playing a less significant role than the attenuation due to absorption in the material used for polarizers, which contributes to the intensity decrease. However, that is not to say that polarization has a negligible effect that we cannot observe. When looking to the percentage changes from sequential runs, we see evidence of how polarization is affected by the shape of the light source. For the circularly shaped light source, the light should be distributed evenly in all directions. For the change from 0 to 20 to 60, the percentage change of all three cases can be argued to be the same because the average of the numbers is 0.568% with a deviation of 0.055%. All three numbers fall within this range. Attenuation is already accounted for since we are comparing the cases that have the same two polarizers attenuating the light so

TABLE III. Wavelengths vs. Intensity and Total Intensity

Wavelength	Light Intensity	Change in Wavelength	Area According to Trapezoidal Method
...	...	...	...
606.401	2.2	2.362	4.9602
608.793	2.3	2.392	5.382
611.216	2.5	2.423	5.8152
613.671	2.6	2.455	6.26025
614.91	2.7	1.239	3.28335
616.158	2.8	1.248	3.432
617.413	2.9	1.255	3.57675
618.677	2.9	1.264	3.6656
619.949	3.1	1.272	3.816
621.23	3.2	1.281	4.03515
622.519	3.3	1.289	4.18925
623.817	3.4	1.298	4.3483
...	...	...	...
Total			3217.82615

naturally the only change in intensity would be from shifting the polarization axis. This is assuming attenuation is the same for all degrees of the polarizer which may not necessarily be true for our polarizers and error is taken into account with the average and standard deviation. In table III and IV, we are comparing intensities for sequential signals polarized by increments of 20 degrees. Therefore, we expect having the same percentage shift when we go from one case to the next one. Indeed the percentage shift is the same within the error bar, except its magnitude, which is smaller than $cos^2(20°)$. This fact is an indicator of the attenuation of light intensity due to absorption in our polarizers, which are clearly far from ideal.

With the square-shaped polygon light, where we would expect to have uneven distribution of light because of its shape, there is no such similar correlation as with the circle light when looking to the percent change in intensity for sequential cases as shown in Table VI.

TABLE IV. Total Intensity and Percent Change of Intensity from Polarized Light Released by a Circularly Shaped Source

	Intensity	% Change
no polarizer	3217.8262	
0 deg	2090.2813	35.041%
20 deg	2100.9022	0.508%
40 deg	2088.7237	0.580%
60 deg	2075.8388	0.617%

Intensity column represents the area below the Planck curve of radiancy from Figure 8.
The % Change is the percentage change between sequential cases, as explained in the main text.

TABLE V. Total Intensity and Percent Change in Intensity from Polarized Light Released by a Polygon Shaped Source

	Intensity	% Change
no polarizer	7244.2025	
0 deg	4948.5262	31.690%
20 deg	5058.8125	2.229%
40 deg	5139.0871	1.587%
60 deg	4908.0799	4.495%

Intensity column represents the area below the Planck curve of radiancy from Figure 9.
The % Change is the percentage change between sequential cases, as explained in the main text.

TABLE VI. Comparision of Circle and Polygon Light Source Sequential Changes

Degree Rotation	Polygon	Scale Factor	Polygon	Circle
20	0.508	4.386	2.229	2.229
40	0.580	2.737	1.587	1.587
60	0.617	7.287	4.495	4.495

The fact that it varies drastically from the results reported for the circularly shaped light source, which is our control case, supports our theory that the square-shaped polygon cutout polarizes the light unevenly in various directions, since it allows more light through in one direction of polarization as opposed to another. This topic is so exciting and consistent with the findings reported in the article "Astronomy gets polarized" by Ron Cowen published in Science News in 2006[13] that we intend to continue developing strong research in this area, with our goal towards a publication in a peer-review journal in 2014.

C. PEA Analysis

The difference in shape between Figure 12 and Figure 13 is mainly due to instrumentation, and in particular to the alignment of the optical components. The right wing of the experimental signal in Figure 13 is diminished by the spectral response of the photo cell, as defined by PASCO®[14], see Figure 17; while the left wing appears to be diminished by attenuation due to the optical components of the set-up - like the lenses and prism - and possibly some Rayleigh scattering which occurs in the sodium lamp.

The uncertainty introduced by our equipment is approximately 1 nm. This relates the 588.299 nm reading on our experimental data reported in Figure 13 to a wavelength between 587.299 nm and 589.299 nm. This correlates perfectly with the 589 nm wavelength listed in the NIST Database[6].

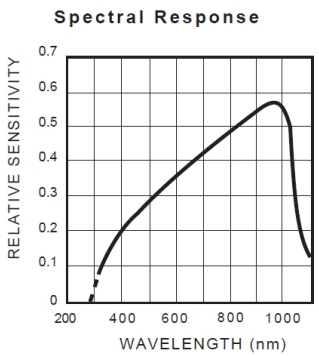

VI. RESULTS AND CONCLUSIONS

The experiments done by our team over the last year have produced interesting and informative results. We have presented our research several times throughout the year. Copies of the abstracts and posters for the South Central Conference for Undergraduate Women in Physics[5], Joint Spring 2013 Meeting of the Texas Sections of the APS, AAPT, SPS[15], Texas Undergraduate Research Day at the Capitol in Austin, Texas[16], and Joint Fall 2013 Meeting of the Texas Sections of the APS, AAPT, SPS[4] are included in Appendix B.

A. HRD Conclusions

We were able to simulate in our lab environment several stars in the main sequence, by using a flame near the thermal equilibrium regime. Simulation of red giants and blue dwarfs proved to be more complicated, as described in the HRD Analysis.

B. APSL Conclusions

It is possible to observe the effects of polarization of light due to the shape of the light source. From our observations, the percentage change between different angular orientations for a polygon shaped light source supports the hypothesis that the shape of even a natural light source indeed polarizes the light before it reaches the first polarizer.

C. PEA Conclusions

It is indeed possible to detect gaseous chemicals via absorption spectra embedded in a blackbody spectrum. Our experiment with sodium, reported above and another measurement using hydrogen, showed that.

VII. FUTURE WORK

A. HRD Future Work

We still very much like the idea of going outside to take measurements of stars in our area. With most of the equipment built and calibration completed, our main issue remains the safety of the optics equipment when transported through the rooftop access. Once the issue will be resolved, we will try to take more data outside.

B. APSL Future Work

We will continue our work on polarization of light due to the shape of the light source. We plan to use a variety of shapes, i.e. an oval, to see if we obtain similar results as with our present experiment. We will work further on data analysis and interpretation in order to refine a method for better separating the attenuation phenomenon from the polarization effect. We intend to submit studies in this topic for publication in a peer-review journal in 2014.

C. PEA Future Work

We will continue to improve the setup by mounting the telescope to an optical bench link in order to eventually take the solar reading. Further work on the theoretical model equations and study of other elements and compounds will also further our understanding.

VIII. EXPENSES

Only those items purchased with the $2,000 funds sponsored by the Sigma Pi Sigma or by the Physics Department are listed on our ledger (Appendix A). Any supplies donated to the project by the members of the research team have been omitted. Expenses exceeding $2000.00 were covered by the Physics Department of Lamar University. Please see an itemized list on page 28.

REFERENCES

[1]The Phillip M. Drayer Department of Electrical Engineering, "Rooftop platform access policy," Tech. Rep. (Beaumont, 2013) private commuincation.

[2]B. Warren, "Seeing and transparency," The Flint River Observer **7** (2004).

[3]C. Bahrim, "Blackbody radiation," (2012), http://sethi.lamar.edu/bahrim-cristian/Courses/PHYS4480/4480-LABS/4480_lab_2.pdf.

[4]K. Townley-Smith, S. Vogler, and C. Bahrim, "Analysis of atomic spectra with applications to solar measurements," in *Bulletin of the American Physical Society*, Joint Fall 2013 Meeting of the Texas Sections of the APS, AAPT, SPS, Vol. 58 (APS, University of Texas at Brownsville, 2013) p. D1.00003.

[5]S. Vogler and C. Bahrim, "Analysis of atomic emission spectra: a refined way to understand the photon concept," in *South Central Conference for Undergraduate Women in Physics* (University of Texas at Austin, 2013).

[6]A. Kramida, Y. Ralchenko, J. Reader, and NIST ASD Team, "NIST atomic spectra database," (2013).

[7]Nathional Weather Service, "Layers of the atmosphere," (2013).

[8]H. E. Smith, "The sun," (1999).

[9]University of Ontario, "Structure and composition of the troposphere," (2013).

[10]D. R. Williams, "Earth fact sheet," Tech. Rep. (Greenbelt, 2013) http://nssdc.gsfc.nasa.gov/planetary/factsheet/earthfact.html.

[11]D. R. Williams, "Sun fact sheet," Tech. Rep. (Greenbelt, 2013) http://nssdc.gsfc.nasa.gov/planetary/factsheet/sunfact.html.

[12]M. A. Green, *Solar Cells: Operating Principles, Technology, and System Applications* (Princeton Hill, Inc., Englewood Cliffs, 1982).

[13]R. Cowen, "Astronomy gets polarized," Science News **170**, 24–25 (2006).

[14]"Ligth sensor and high sensitivity light sensor: Instruction sheet for the pasco model ci-6504a and model ci-6604," Tech. Rep. (Roseville, 1997) http://www.pasco.com/file_downloads/product_manuals/Light-Sensor-Manual-CI-6504A.pdf.

[15]S. Vogler, K. Townley-Smith, and C. Bahrim, "Analysis of atomic emission spectroscopy: a refined way to understand the photon concept." in *Bulletin of the American Physical Society*, Joint Spring 2013 Meeting of the Texas Sections of the APS, AAPT, SPS, Vol. 58

(APS, Tarleton State University, 2013) p. K1.00008.

[16]S. Vogler and C. Bahrim, "Analysis of atomic emission spectra with applications in the study of our universe," in *Texas Undergraduate Research Day at the Capitol* (Council of Public University Presidents and Chancellors, Austin, 2013) paper #10 in the Proceedings.

Appendix A: Expense Detail

Ledger	
Tripod (PlatinumPlus by Sunpak Ultra)	$89.99
Neon Cord (Rope for hoisting equipment)	$5.96
Heavy Duty Bins For hoisting equipment (BIN,HVYDTY,21)	$65.98
Mobile Clear Box For hoisting small equipment (BOX,MOBILE,CLR)	$12.99
PVC Pipe for Telescope-Fiber Adapter (1-IN X 5-FT SCH-40 PVC PI)	$5.74
Dowel Rod for Telescope-Fiber Adapter (1"X48"DOWEL ROD	$7.94
Epoxy for Telescope-Fiber Adapter (.47 OZ EPOXY INSTANT MIX)	$3.77
Tent for light shield (FRP TENT)	$29.97
Play-Doh For molding adapters (SECONDARY)	$5.92
Basic Optics Prism Spectrophotometer Kit (OS-8544) Basic Optics Prism Mount (OS-8543) Basic Optics Black Body Light Source (OS-8542) DataStudio Experiment Setup CD	$344.35
Basic Optics Education Spectrophotometer Accessory (OS-8537) Collimating Slits Collimating Lens Diffraction Grating Focusing Lens	$639.23
Aperture Bracket (OS-8534A)	$86.33
Infrared Sensor (CI-6628)	$222.13
UVA Light Sensor (CI-9784)	$173.63
High Sensitivity Light Sensor (CI-6604)	$134.83
Basic Optics Polarizer Set (OS-8473) Two Polarizer Disks Optics Holder	$57.23
2-Axis Fiber Alignment Mount w/ Standard Kinetic Movement (55476)	$379.05
Fiber Optic Cable (57060)	$26.60
Fiber Optic Cable Hot Knife (54014)	$141.55
Total	**$2433.19**

Appendix B: Research Presentations

1. South Central Conference for Undergraduate Women in Physics (University of Texas at Austin, 2013)

Analysis of Atomic Emission Spectra: a refined way to understand the photon concept

Sara-jeanne Vogler, Cristian Bahrim

Department of Physics, Lamar University, Beaumont, TX 77710-10046

Spectroscopic analysis of atoms and simple molecules reveals the atomic structure, the emission of photons, and the quantum interaction between light and matter. The photon emission obeys the selection rules for orbital and spin angular momenta, the parity and the linear momentum conservation laws. One can identify the constituents of matter by finding the characteristic photons emitted by gaseous discharges. The significance of such knowledge impacts areas from metallurgy to stellar observation.

Our discharge tubes allow the emitted photon to broaden to a few nm width and so we can better resolve the emission lines. From the FWHM we find the uncertainty in the energy value of the atomic excited states. From the relative intensity of the emission lines, de-convoluted from the Maxwell-Boltzmann distribution in discharges at thermal equilibrium, we can find the effective temperature of atoms and their average speed. Pressure **broadening** reveals the quantum characteristics of photon emission by including the uncertainty principle. From the Lorentzian profile of each photon the lifetime of the atomic states can be estimated.

2. Joint Spring 2013 Meeting of the Texas Sections of the APS, AAPT, SPS

Abstract Submitted
for the TSS13 Meeting of
The American Physical Society

Analysis of Atomic Emission Spectra: a refined way to understand the photon concept[1] SARA-JEANNE VOGLER, KEELEY TOWNLEY-SMITH, CRISTIAN BAHRIM, Lamar University — Spectroscopic analysis of atoms and simple molecules reveals the atomic structure, the emission of photons, and the quantum interaction between light and matter. The optics equipment allows us to resolve the emission lines with a precision better than 1 nm. Pressure broadening effect enlarges the emission lines of our light sources to several nm at FWHM. From the relative intensity of the emission lines, de-convoluted using the Maxwell-Boltzmann distribution of atoms in a gaseous discharge at thermal equilibrium, we can find the effective temperature of the atoms and their average speed. Pressure broadening reveals the quantum characteristics of the photon emission by including the uncertainty principle. From the Lorentzian profile of each photon one can find the lifetime of the atomic states in given experimental conditions, and by comparison with their natural lifetime, the effect of the collisional de-excitation can be estimated. Because the photon emission obeys the selection rules for orbital angular momentum, spin, and parity, one can identify the characteristic wavelengths of the atomic constituents of light sources. We are going to present a brief progress report on the applications of the spectroscopic analysis in stellar measurements done under our 2013 Sigma Pi Sigma Undergraduate Research Award.

[1]Project done under the NSF DUE 0757057 grant and the 2013 Sigma Pi Sigma Undergraduate Research Award.

Cristian Bahrim
Lamar University

Date submitted: 04 Mar 2013 Electronic form version 1.4

Analysis of Atomic Emission Spectra: a refined way to understand the photon concept

Sara-Jeanne Vogler and Cristian Bahrim
Department of Physics, Lamar University, Beaumont, TX 77710-10046

Scope

Spectroscopic analysis of atoms and simple molecules reveals the atomic structure, the emission of photons, and the quantum interaction between light and matter. The analysis of emission lines is possible with our equipment by allowing the pressure broadening effect to enlarge these lines to a few nm in width.

Background

The photon emission obeys the selection rules for orbital angular momentum, spin, and parity (because the photon transports linear momentum). One can identify the constituents of matter (atoms, molecules, impurities) by finding the characteristic photons emitted by gaseous discharges.

Selection Rules

$\Delta L = 0, \pm 1$

Parity changes

$\Delta S = 0$

Calibration

The setup was calibrated using hydrogen. The spectra for all gases were excited using the same equipment and all measurements were taken at thermal equilibrium. This allows the assumption that all gases measured have the same effective temperature.

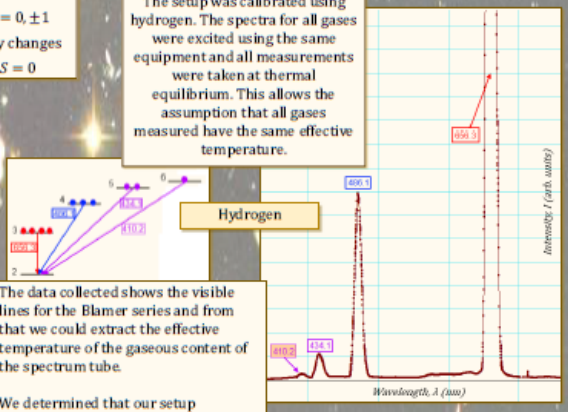

The data collected shows the visible lines for the Blamer series and from that we could extract the effective temperature of the gaseous content of the spectrum tube.

We determined that our setup

a) has a precision of
0.8 nm

b) allows us to reach a thermal equilibrium at
T = 2800 K ± 9%

c) equivalent to a kinetic energy of
<K> = 0.24 eV

Experimental Setup and Procedure

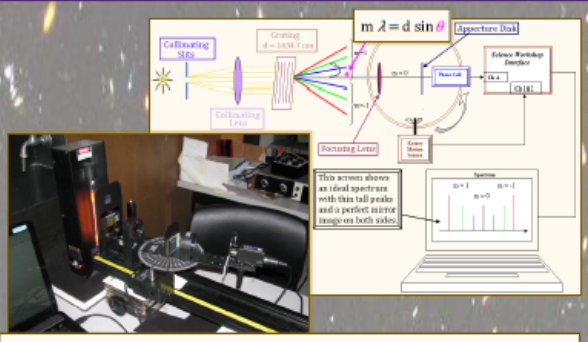

From the relative intensity of the emission lines, de-convoluted from the Maxwell-Boltzmann distribution in discharges at thermal equilibrium, we can find the effective temperature of atoms and their average speed.

$$\frac{I}{I'} = exp\left[\frac{hc}{kT}\left(\frac{1}{\lambda'} - \frac{1}{\lambda}\right)\right] \qquad \langle K \rangle = kT \qquad \langle K \rangle = \frac{1}{2}mv^2$$

Reported to the right

Pressure broadening reveals the quantum characteristics of photon emission by including the uncertainty principle. From the Lorentzian profile of each photon the lifetime of the atomic states can be estimated.

$$\Delta t = \frac{1}{\Delta \nu} \qquad \Delta \nu = \frac{\Delta\lambda \cdot c}{\lambda^2}$$

Reported below

From the FWHM we find the uncertainty in the energy value of the atomic excited states.

$$\Delta E = \frac{\hbar}{\Delta t}$$

Reported below

Knowing the spectrum for helium allows us to identify the impurities in the discharge tube and the minor defects of our setup.

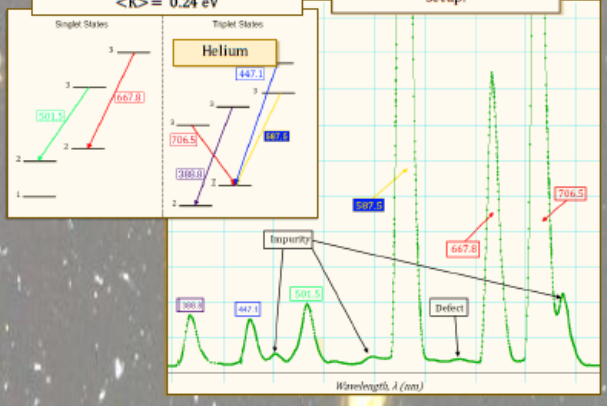

Results

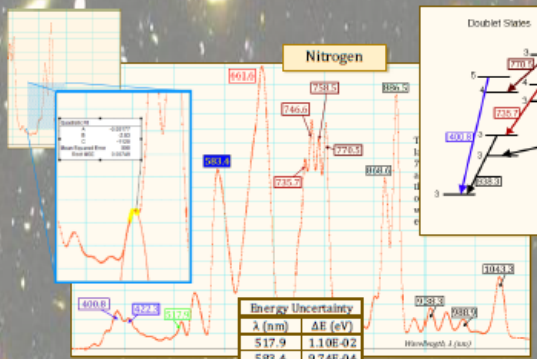

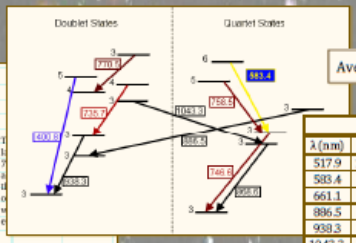

Average speed = 1810 m/s

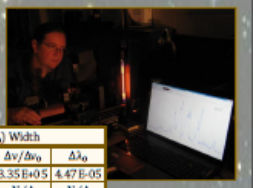

Experimental ($\Delta\nu$) and Natural ($\Delta\nu_0$) Width

λ (nm)	Δλ	Δν (Hz)	Δt (sec)	$\Delta\nu_0$	$\Delta\nu/\Delta\nu_0$	$\Delta\lambda_0$
517.9	15.0	1.68E+13	5.97E-14	5.00E+07	3.35E+05	4.47E-05
583.4	1.7	1.48E+12	6.76E-13	N/A	N/A	N/A
661.1	0.7	4.53E+11	2.21E-12	6.01E+07	7.53E+03	8.76E-05
886.5	0.3	1.08E+11	9.28E-12	9.80E+04	1.10E+06	2.57E-07
938.3	2.1	7.23E+11	1.38E-12	1.36E+07	5.32E+04	3.99E-05
1043.3	1.3	3.51E+11	2.85E-12	1.80E+02	1.95E+09	6.54E-10

Energy Uncertainty

λ (nm)	ΔE (eV)
517.9	1.10E-02
583.4	9.74E-04
661.1	2.98E-04
886.5	7.09E-05
938.3	4.76E-04
1043.3	2.31E-04

References

NASA; ESA; G. Illingworth, D. Magee, and P. Oesch, *eXtreme Deep Field*. [2010 July 21]. University of California, Santa Cruz; R. Bouwens, Leiden University; and the HUDF09 Team.

Kramida, A., Ralchenko, Yu., Reader, J., and NIST ASD Team (2012). *NIST Atomic Spectra Database (ver. 5.0)*. [Online]. Available: http://physics.nist.gov/asd [2013, January 13]. National Institute of Standards and Technology, Gaithersburg, MD.

Reader, Joseph. (1980). *Wavelengths and Transition Probabilities for Atoms and Atomic Ions NSRDS-NBS 68*. http://www.nist.gov/data/nsrds/NSRDS-NBS-68.pdf [2013, January 13]. U.S. Dept. of Commerce, National Bureau of Standards, Washington, DC.

Research sponsored by an NSF – STEP program called "STARSTEP":
Students Advancing through Involvement in Research Student Talent Expansion Program

3. Texas Undergraduate Research Day at the Capitol in Austin, Texas

10. Lamar University

Sara-Jeanne Vogler

ANALYSIS OF ATOMIC EMISSION SPECTRA WITH APPLICATIONS IN THE STUDY OF OUR UNIVERSE

Faculty Advisor: Cristian Bahrim, PhD

Spectroscopic analysis of atoms and simple molecules reveals their atomic structure. The analysis of emission lines is possible with PASCO® equipment by allowing the pressure broadening effect to enlarge these lines to a few nm in width. The photon emission obeys the selection rules for orbital angular momentum, spin, and parity. One can identify the constituents of matter by finding the characteristic photons emitted by gaseous discharges. From the relative intensity of the emission lines, de-convoluted from the Maxwell- Boltzmann distribution in discharges at thermal equilibrium, the effective temperature of atoms and their average speed is found. From the Lorentzian profile of each photon the lifetime of the atomic states can be estimated. From the FWHM the uncertainty in the energy value of the atomic excited states is found. This theoretical knowledge can be applied to absorption spectra as well as precisely identifying wavelength with the goal to determine the life cycle of bright stars, for studying the influence of the atmospheric constituents on the stellar and solar spectra, and also for testing the effects of optical instruments on astronomic measurements.

Analysis of Atomic Emission Spectra with Applications in the Study of our Universe

Sara-Jeanne Vogler and Cristian Bahrim
Department of Physics, Lamar University, Beaumont, TX 77710-10046

Atomic Spectroscopy: Principles and Characteristics of Atomic Samples

Scope and Background

Spectroscopic analysis of atoms and simple molecules reveals the atomic structure, the emission of photons, and the quantum interaction between light and matter. The analysis of emission lines is possible with our equipment by allowing the pressure broadening effect to enlarge these lines to a few nm in width.

The photon emission obeys the selection rules for orbital angular momentum, spin, and parity. One can identify the constituents of matter (atoms, molecules, impurities) by finding the characteristic photons emitted by gaseous discharges.

Description of Property	Change in Property	Characteristic of the Photon
Spin (S)	$\Delta S = 0$	A photon has no mass, and therefore no center of mass to spin around.
Orbital Rotational Momentum (L)	$\Delta L = 0, \pm 1$	Change of the orbit by one $\hbar$ increment. It only equals zero in multiple electron systems due to the electrons' delocalization.
Parity (π)	$\Delta \pi = \pm 1$	A photon carries linear momentum that pushes back (recoils) on the atom as it escapes.

Experimental Setup

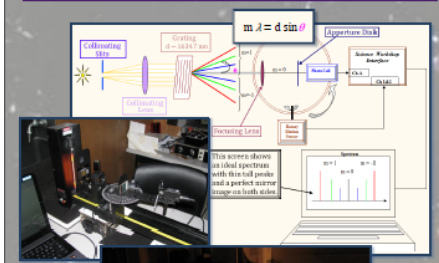

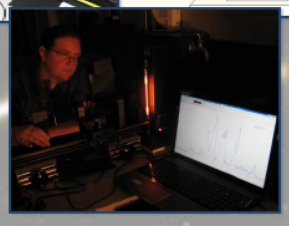

Characteristic Parameters

From the relative intensity of the emission lines, which indicates the Maxwell-Boltzmann distribution of atoms on excited states in gaseous discharges at thermal equilibrium,

$$\frac{I}{I'} = exp\left[\frac{hc}{kT}\left(\frac{1}{\lambda} - \frac{1}{\lambda'}\right)\right]$$

we can find the effective temperature of atoms

$$\langle K \rangle = kT$$

Reported below

and their average speed.

$$v = \sqrt{\frac{2}{m}\langle K \rangle}$$

Reported below

Pressure broadening reveals the quantum characteristics of photon emission by including the uncertainty principle. From the Lorentzian profile of each photon (short duration wave train) the lifetime of the atomic states can be estimated.

$$\Delta\nu = \frac{\Delta\lambda \cdot c}{\lambda^2} \qquad \Delta t = \frac{1}{\Delta\nu}$$

From FWHM of the emission lines we find the uncertainty in the energy value of the atomic excited states.

$$\Delta E = \frac{h}{\Delta t}$$

Calibration and General Characteristics

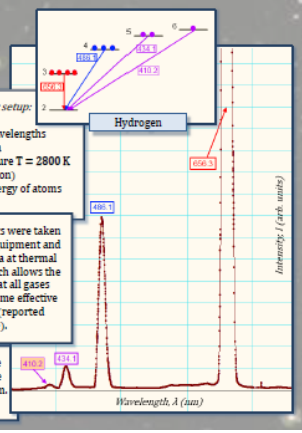

Characteristics of our setup:

a) Precision in the wavelengths measured ~ 0.8 nm
b) Effective temperature T = 2800 K (with a 9% precision)
c) Average kinetic energy of atoms $\langle K \rangle$ = 0.24 eV

All measurements were taken with the same equipment and of gaseous media at thermal equilibrium, which allows the assumption that all gases used have the same effective temperature (reported above).

The labels of emission lines are color coded consistent with the color used in the actual spectrum. For example, 656.3 nm is red.

Atomic Composition of Complex Media from the Emission Lines

Data Analysis: Hunting for Impurities

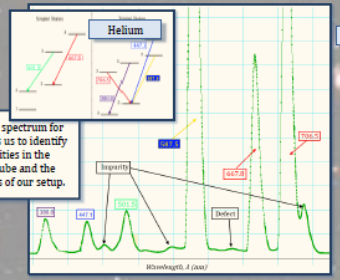

Knowing the spectrum for helium allows us to identify the impurities in the discharge tube and the minor defects of our setup.

Spectral Analysis of Pure Water (H_2O)

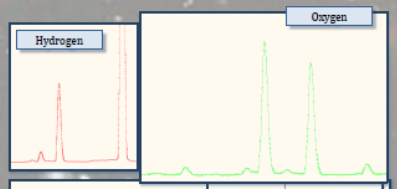

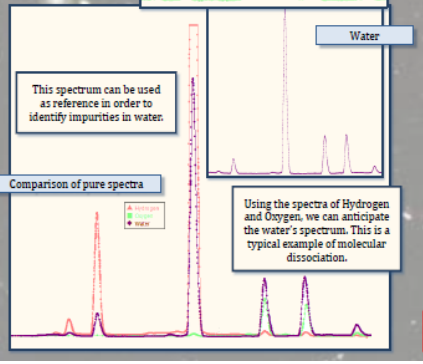

This spectrum can be used as reference in order to identify impurities in water.

Comparison of pure spectra

Using the spectra of Hydrogen and Oxygen, we can anticipate the water's spectrum. This is a typical example of molecular dissociation.

The Study of the Chemical Composition of Air

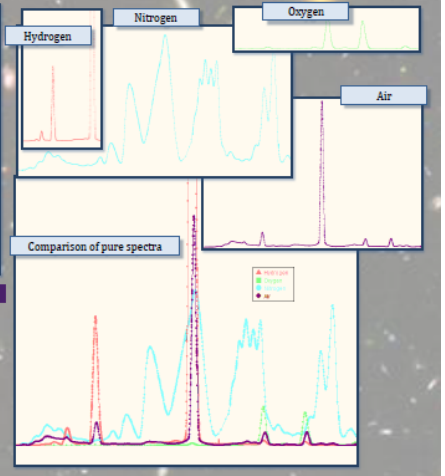

Work in Progress

This theoretical knowledge is being applied to a ΣΠΣ Undergraduate Research Award received by the Lamar University chapter of the Society of Physics Students to analyze the life cycle of bright stars, study the constituents of the atmosphere, and test the effects of optical instruments on astronomic measurements.

References

NASA; ESA; G. Illingworth, D. Magee, and P. Oesch, *eXtreme Deep Field* (2010 July 21). University of California, Santa Cruz; R. Bouwens, Leiden University; and the HUDF09 Team.

Kramida, A., Ralchenko, Yu., Reader, J., and NIST ASD Team (2012). *NIST Atomic Spectra Database* (ver. 5.0), [Online]. Available: http://physics.nist.gov/asd [2013, January 13]. National Institute of Standards and Technology, Gaithersburg, MD

Reader, Joseph, (1980). *Wavelengths and Transition Probabilities for Atoms and Atomic Ions NSRDS-NBS 68*. http://www.nist.gov/data/nsrds/NSRDS-NBS-68.pdf [2013 , January 11]. U.S. Dept. of Commerce, National Bureau of Standards, Washington, DC.

Research sponsored by an NSF – STEP program called 'STAIRSTEP':
Students Advancing through Involvement in Research Student Talent Expansion Program

4. Joint Fall 2013 Meeting of the Texas Sections of the APS, AAPT, SPS

Abstract Submitted
for the TSF13 Meeting of
The American Physical Society

Analysis of Atomic Spectra with applications to solar measurements[1] KEELEY TOWNLEY-SMITH, SARA-JEANNE VOGLER, CRISTIAN BAHRIM, Department of Physics, Lamar University — Atomic and molecular spectroscopy allows us to reveal the constituents of matter. Using PASCO® equipment we analyze the emission lines of several components of air such as oxygen, hydrogen, nitrogen, carbon dioxide, water, and helium. The pressure broadening on the emission lines allows us to enlarge them to a few nm in width and thus, to well resolve the lines. The characterization of the emission lines is applied to unknown compound spectra to identify the atomic constituents present. Also, the information can be further used to identify absorption lines embedded in the emission spectra of a known blackbody source of radiation: indeed the profile of the emission lines and their location should coincide with the absorption lines. The dominant absorption lines are from the ground atomic state. We attempt to apply this knowledge to de-convolute the absorption lines from the blackbody spectrum of the Sun modified by the absorption lines of Hydrogen and Helium atoms located in the Sun's corona, and of Nitrogen, Oxygen, Carbon and other atoms from the Earth's atmosphere.

[1]We acknowledge the Sigma Pi Sigma organization of AIP for sponsoring our Lamar University SPS Chapter's project on astronomical and solar measurements.

Cristian Bahrim
Department of Physics, Lamar University

Date submitted: 12 Sep 2013 Electronic form version 1.4

Analysis of Atomic Spectra with Applications to Solar Measurements

Keeley Townley-Smith, Sara-Jeanne Vogler and Cristian Bahrim
Department of Physics, Lamar University, Beaumont, TX 77710-10046

LAMAR UNIVERSITY

Scope and Background

Spectroscopic analysis of atoms and simple molecules reveals the atomic structure, the characteristic photons for each element, and the quantum interaction between light and matter. The analysis of emission lines is possible with our equipment by allowing the pressure broadening effect to enlarge these lines to a few nm in width.

The photon emission obeys the selection rules for orbital angular momentum, spin, and parity (because the photon transports linear momentum). One can identify the constituents of matter (atoms, molecules, impurities) by finding the characteristic photons emitted by gaseous discharges.

Description of Property	Change in Property	Characteristic of the Photon
Spin (S)	$\Delta S = 0$	A photon has no mass, and therefore no center of mass to spin around.
Orbital Rotational Momentum (L)	ΔL	Change of the orbit by one $\hbar$ increment. It only equals zero in multiple electron systems due to the electrons' delocalization.
Parity (π)	$\Delta\pi = \pm 1$	A photon carries linear momentum that pushes back (recoils) on the atom as it escapes.

Experimental Setup and Procedure

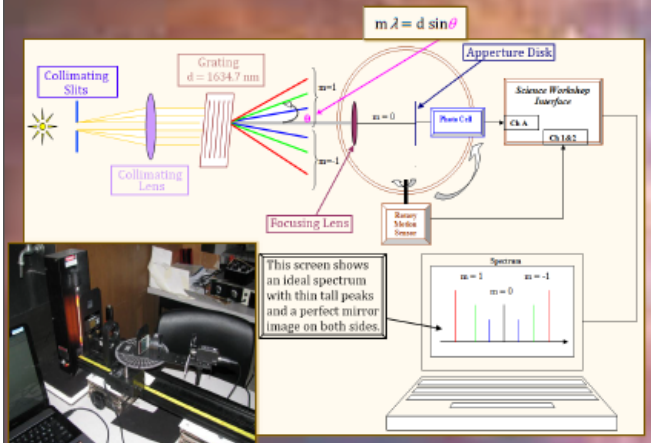

This screen shows an ideal spectrum with thin tall peaks and a perfect mirror image on both sides.

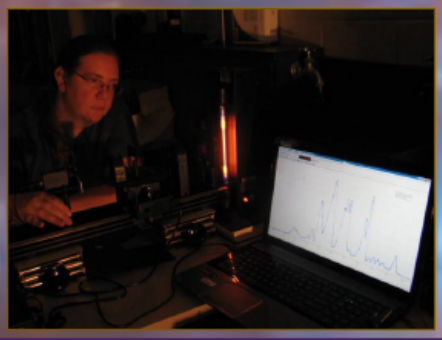

The Study of the Chemical Composition of Air

Using PASCO equipment we analyze the emission lines of several components of air such as oxygen, hydrogen, nitrogen, carbon dioxide, water, and helium (below are a few examples).

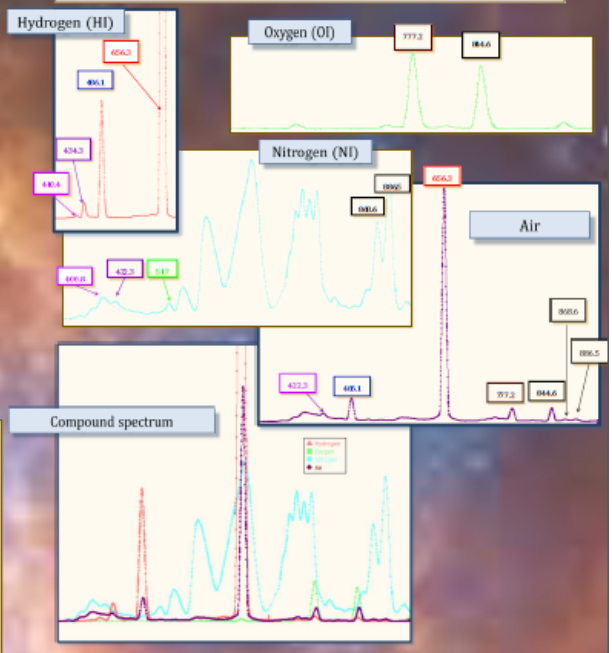

Absorption lines embedded in Sun's radiation spectrum

We identify the absorption lines embedded in the emission spectrum of the Sun by comparison with the position and amplitude of the emission lines in the pure discharge spectra of most common gases.

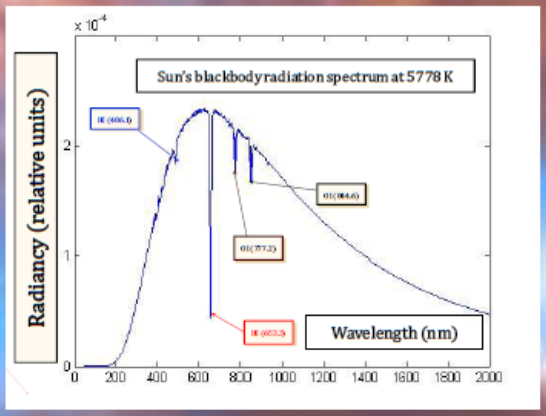

Bibliography

NASA; ESA; G. Illingworth, D. Magee, and P. Oesch, *eXtreme Deep Field* [2010 July 21]. University of California, Santa Cruz; R. Bouwens, Leiden University; and the HUDF09 Team.

Kramida, A., Ralchenko, Yu., Reader, J., and NIST ASD Team (2012). *NIST Atomic Spectra Database (ver. 5.0)*, [Online]. Available: http://physics.nist.gov/asd [2013, January 13]. National Institute of Standards and Technology, Gaithersburg, MD

Reader, Joseph. (1980). *Wavelengths and Transition Probabilities for Atoms and Atomic Ions NSRDS-NBS 68*. http://www.nist.gov/data/nsrds/NSRDS-NBS-68.pdf [2013, January 11]. U.S. Dept. of Commerce, National Bureau of Standards, Washington, DC.

We acknowledge the Sigma Pi Sigma organization of AIP for sponsoring our Lamar University SPS Chapter's project on astronomical and solar measurements and the NSF Grant 0757057 (STAIRSTEP).

SIGMA PI SIGMA
The Physics Honor Society